

2
MASTER

DISCLAIMER

This book was prepared as an account of work sponsored by an agency of the United States Government. Neither the United States Government nor any agency thereof, nor any of their employees, makes any warranty, express or implied, or assumes any legal liability or responsibility for the accuracy, completeness, or usefulness of any information, apparatus, product, or process disclosed, or represents that its use would not infringe privately owned rights. Reference herein to any specific commercial product, process, or service by trade name, trademark, manufacturer, or otherwise does not necessarily constitute or imply its endorsement, recommendation, or favoring by the United States Government or any agency thereof. The views and opinions of authors expressed herein do not necessarily state or reflect those of the United States Government or any agency thereof.

HEDL - SA-1966 - FP
CONF - 800607-67

SODIUM LOOP SAFETY FACILITY W-2 EXPERIMENT
FUEL PIN RUPTURE DETECTION SYSTEM

M. A. Hoffman
T. L. Kirchner
S. C. Meyers

May 1980

Hanford Engineering Development Laboratory

HANFORD ENGINEERING DEVELOPMENT LABORATORY
Operated by Westinghouse Hanford Company, a subsidiary of
Westinghouse Electric Corporation, under the Department of
Energy Contract No. DE-AC14-76FF02170

gb
COPYRIGHT LICENSE NOTICE

By acceptance of this article, the Publisher and/or recipient acknowledges the U.S. Government's right to retain a nonexclusive, royalty-free license in and to any copyright covering this paper.

DISTRIBUTION OF THIS DOCUMENT IS UNLIMITED

DISCLAIMER

This report was prepared as an account of work sponsored by an agency of the United States Government. Neither the United States Government nor any agency Thereof, nor any of their employees, makes any warranty, express or implied, or assumes any legal liability or responsibility for the accuracy, completeness, or usefulness of any information, apparatus, product, or process disclosed, or represents that its use would not infringe privately owned rights. Reference herein to any specific commercial product, process, or service by trade name, trademark, manufacturer, or otherwise does not necessarily constitute or imply its endorsement, recommendation, or favoring by the United States Government or any agency thereof. The views and opinions of authors expressed herein do not necessarily state or reflect those of the United States Government or any agency thereof.

DISCLAIMER

Portions of this document may be illegible in electronic image products. Images are produced from the best available original document.

CONTENTS

	<u>Page</u>
Figures	iv
Tables	v
1.0 INTRODUCTION	1
1.1 SODIUM LOOP SAFETY FACILITY (SLSF) W-2 TEST AND OBJECTIVES	1
1.2 FUEL PIN RUPTURE DETECTION SYSTEM (FPRDS)	1
2.0 FUEL PIN RUPTURE DETECTION SYSTEM DESCRIPTION	5
2.1 ACOUSTIC WAVEGUIDE DESIGN AND MATERIALS SELECTION	5
2.1.1 Calculation of Rupture Lateral Locations	5
2.1.2 Acoustic Wave Propagation	14
2.1.3 Reflection and Critical Angle Effects On Acoustic Waveguide Design	15
2.1.4 Acoustic Waveguide Design	17
2.2 HIGH TEMPERATURE, SODIUM IMMERSIBLE MICROPHONES	24
2.3 ELECTRONICS SYSTEM DESCRIPTION	29
3.0 TESTING RESULTS	33
3.1 ATTENUATION COMPARISONS FOR WAVEGUIDES	33
3.2 CALIBRATION/TEST MODULES	35
4.0 CURRENT STATUS OF THE SLSF W-2 TEST AND FPRDS	39
5.0 CONCLUSION	40
6.0 REFERENCES	41

FIGURES

<u>Figure</u>		<u>Page</u>
1	Fuel Pin Rupture Detection System for SLSF W-2 Test	6
2	Fuel Pin Time Differential Relationships	9
3	Fuel Pin Rupture Location Relationships	11
4	Critical Angle Definition	16
5	Acoustic Pipe Fabrication Details	23
6	Sectional Views of ANL HT Microphone	26
7	HT Microphone and Matchine Core	27
8	Frequency Response of Typical ANL HT Microphone	28
9	FPRDS Electronics Block Diagram	31
10	Typical Transducer Response	32
11	Test Set-Up For Attenuation Comparisons	34
12	Molybdenum Wire Testing	36
13	Molybdenum Wire Testing	37
14	Molybdenum Wire Testing	38

TABLES

<u>Table</u>		<u>Page</u>
1	SLSF W-2 Experiment Objectives	2
2	Fuel Pin Rupture Detection System Features	4
3	FPDRS Components and Functions	7
4	Acoustic Waveguide Design Requirements	18
5	Acoustic Velocities of Selected Materials	18
6	Selected Reflection Coefficients	19
7	Critical Angle For Selected Materials	21
8	Acoustic Waveguide Design Features	22
9	Operating Characteristics of ANL High-Temperature Microphone	25

SODIUM LOOP SAFETY FACILITY W-2 EXPERIMENT
FUEL PIN RUPTURE DETECTION SYSTEM

1.0 INTRODUCTION

1.1 SODIUM LOOP SAFETY FACILITY (SLSF) W-2 TEST AND OBJECTIVES

The objective of the Sodium Loop Safety Facility (SLSF) W-2 experiment is to characterize the combined effects of a preconditioned full-length fuel column and slow transient overpower (TOP) conditions on breeder reactor (BR) fuel pin cladding failures. The W-2 experiment will meet this objective by providing data in two technological areas: 1) time and location of cladding failure, and 2) early post-failure test fuel behavior.

The test involves a seven pin, prototypic full-length fast test reactor (FTR) fuel pin bundle which will be subjected to a simulated unprotected 5¢/s reactivity transient overpower event. The inner, center pin in the bundle will be failed during the overpower event. The outer six pins will provide the necessary prototypic thermal-hydraulic environment for the center pin. The six pins are fabricated with lower enrichments and a larger fuel-to-cladding gap to delay cladding failure during the overpower and insure the center pin fails first. Table 1 summarizes the experiment objectives and features of the SLSF W-2 test.

The fuel pins will be structurally preconditioned by in-situ irradiation at a high specific power level prior to initiating the TOP conditions.

1.2 FUEL PIN RUPTURE DETECTION SYSTEM (FPRDS)

To meet objectives stated previously in Section 1.1, a detection scheme is required to:

- gather acoustic data at the fuel pin bundle,
- detect fuel pin rupture, and
- determine the rupture location.

TABLE 1
SLSF W-2 EXPERIMENT OBJECTIVES

Determine effects of a TOP driven failure on a full length pre-conditioned FTR fuel pin

Monitor acoustic behavior of fuel bundle before and after the rupture

Determine time and location of cladding failures

Monitor early post-failure test fuel behavior

Normally, an acoustic microphone would be placed in sodium adjacent to the fuel pin cladding. In this test, adequate space is not available to locate the acoustic microphone next to the fuel pin; therefore, two high-temperature microphones will be placed 4.57 to 6.09 meters (15 to 20 feet) from the fuel bundle. Each microphone will be remotely fed by an acoustic waveguide attached to the top or bottom of the test fuel pin. The time-differential from the acoustic rupture data will be measured by comparing the analog responses at the microphones. Finally, this time-differential will be used to calculate the actual rupture location.

This scheme, referred to as the Fuel Pin Rupture Detection System (FPRDS) will include the following advanced features:

- Continuous monitoring of the acoustic energy generated by the center fuel pin and its environments;
- Use of two acoustic waveguides (one each attached to the top and bottom of the center fuel pin) to transmit the acoustic energy to the top of the SLSF W-2 test train;
- Use of two high temperature, sodium immersible microphones to receive the transmitted acoustic energy from the waveguides, convert the acoustic signals to electrical signals, and transmit the signals out of the test train to the data acquisition system;
- Use of a high speed FM recorder to record all acoustic data transmitted from both ends of the fuel pin during the test; and
- Use of an advanced, electronics package which will detect the rupture of the fuel pin during the transient and determine and display the rupture location and time.

Features of the FPRDS are summarized in Table 2.

TABLE 2
FUEL PIN RUPTURE DETECTION SYSTEM FEATURES

Remotely located high temperature microphone coupled to the fuel pin with waveguides

High speed recording of acoustic emission before, during, and after the transient

Determination of rupture location and time using advanced electronics package

2.0 FUEL PIN RUPTURE DETECTION SYSTEM DESCRIPTION

The general system configuration is shown in Figure 1. Basic components in the system are:

- Two acoustic waveguides
- Two high temperature, sodium immersible microphones
- Two sets of signal conditioning and recording electronics, and a rupture location determination electronics package.

Component functions and special features are also summarized in Table 3.

2.1 ACOUSTIC WAVEGUIDE DESIGN AND MATERIALS SELECTION

The function of the acoustic waveguide is to transmit any acoustic energy originating in the center fuel pin to the remotely located microphone. The signal must be transmitted with minimal distortion and attenuation within the test train environment. The energy must be transmitted in a manner such that the time dependent nature, frequency, and relative amplitude of the signal is not distorted. Also, the transmitted acoustic energy must be isolated from acoustic signals transmitted along paths other than that of the waveguide acoustic conductor.

To design the acoustic waveguides, it is necessary to identify the manner in which the time difference data is analyzed to determine the failure location. It is also necessary to determine how acoustic energy is transmitted through the waveguide and which parameters effect efficient, accurate transmission of the signal. Finally, the waveguides must satisfy the environmental and dimensional constraints of the test train.

2.1.1 Calculation of Rupture Lateral Locations

During TOP testing of SLSF W-2, the center fuel pin is expected to rupture due to its enriched fuel mixture and higher power generation. The rupture

FUEL PIN RUPTURE DETECTION SYSTEM FOR SLSF W-2 TEST

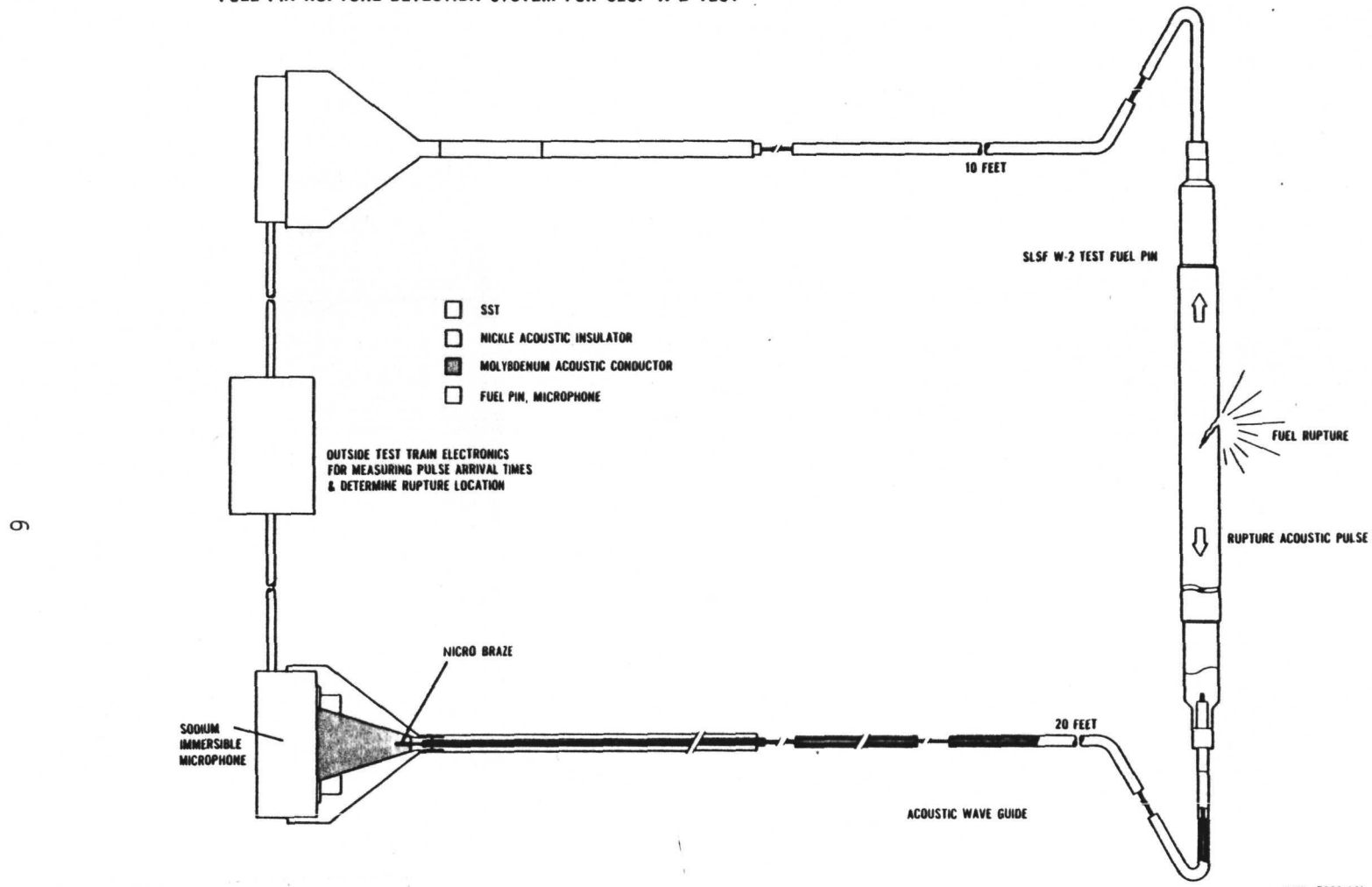


FIGURE 1. Fuel Pin Rupture Detection System for SLSF W-2 Test.

TABLE 3
FPRDS COMPONENTS AND FUNCTIONS

Acoustic Waveguide:	Transmission of acoustic energy from fuel pin end caps to microphone.
High Temperature, Sodium Immersible Microphone:	Conversion of acoustic energy to electrical signal.
Electronics Package:	Recording of converted acoustic information and determination of rupture time and location.

will create a spectrum of acoustic noise. This acoustic noise will travel laterally along the fuel pin toward the end caps. Figure 1 graphically shows this occurrence. Depending upon the rupture location, the acoustic pulse will reach one end cap before the other. The rupture information will then be transmitted to the microphones through the acoustic waveguides. Note that the acoustic waveguides are different lengths and the pin sits vertically in the W-2 test vehicle. Since the microphones are remotely located together, the distance from the bottom fuel pin end cap is greater than the distance from the top end cap.

The objective is to measure the time-differential (Δt) at the end caps. Since the acoustic waveguide distances and material characteristics will be known, the Δt can be calculated. Figure 2 shows the physical parameters needed, where:

x, y = lateral location distances of rupture
 v_x, v_y = mean velocities along x & y distances
 L = known length of fuel pin
 D_1, D_2 = actual known length of waveguide
 v_1, v_2 = mean velocities along D_1 & D_2
 t_1, t_2 = Lapse time of rupture data at end of D_1 & D_2

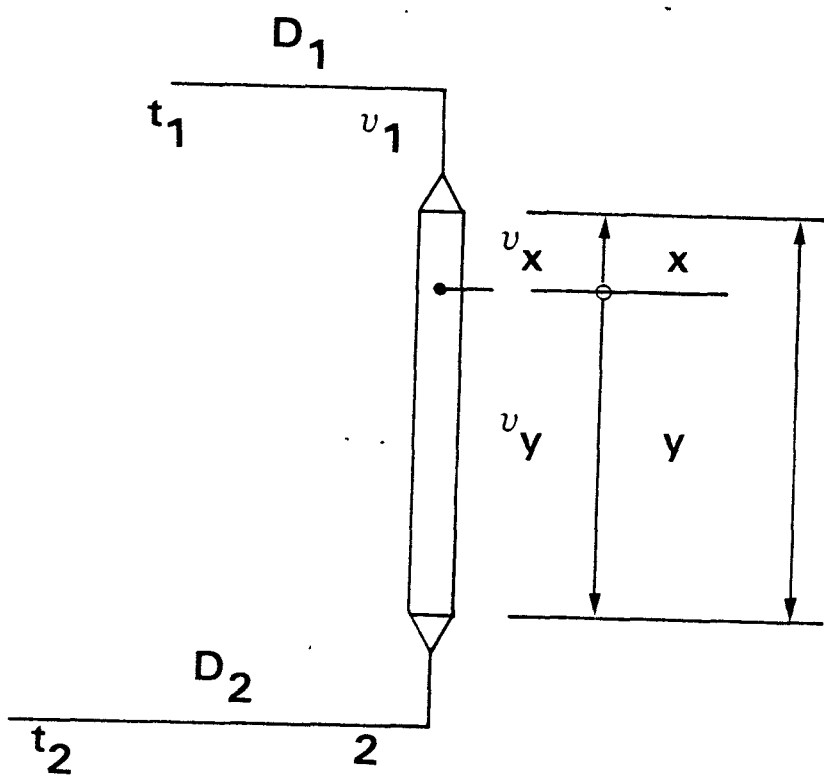
Since all quantities except x, y, t_1 , and t_2 are known, the following relationship applies:

$$x + y = L$$

$$t_1 = x/v_x + D_1/v_1$$

$$t_2 = y/v_y + D_2/v_2$$

$$t_1 - t_2 = \Delta t = x/v_x + D_1/v_1 - y/v_y - D_2/v_2$$



HEDL 8005-155 7

FIGURE 2. Fuel Pin Time Differential Relationships.

$$\Delta t = x/v_x + D_1/v_1 - \frac{(L - x)}{v_y} - D_2/v_2$$

$$\Delta t = x/v_x + x/v_y + D_1/v_1 - D_2/v_2 - L/v_y$$

$$\Delta t = \frac{(v_x + v_y)x}{v_x v_y} + \frac{D_1}{v_1} - \frac{D_2}{v_2} - L/v_y$$

$$\therefore x = \left[\Delta t + \frac{D_2}{v_2} - \frac{D_1}{v_1} + L/v_y \right] \frac{v_x v_y}{(v_x + v_y)^2} \quad (1-1)$$

Measuring t , the rupture location can be calculated. This calculation assumes the temperature for segments x , y , 1, and 2 are constant over the segment length. Figure 3 graphically shows all the above relationships.

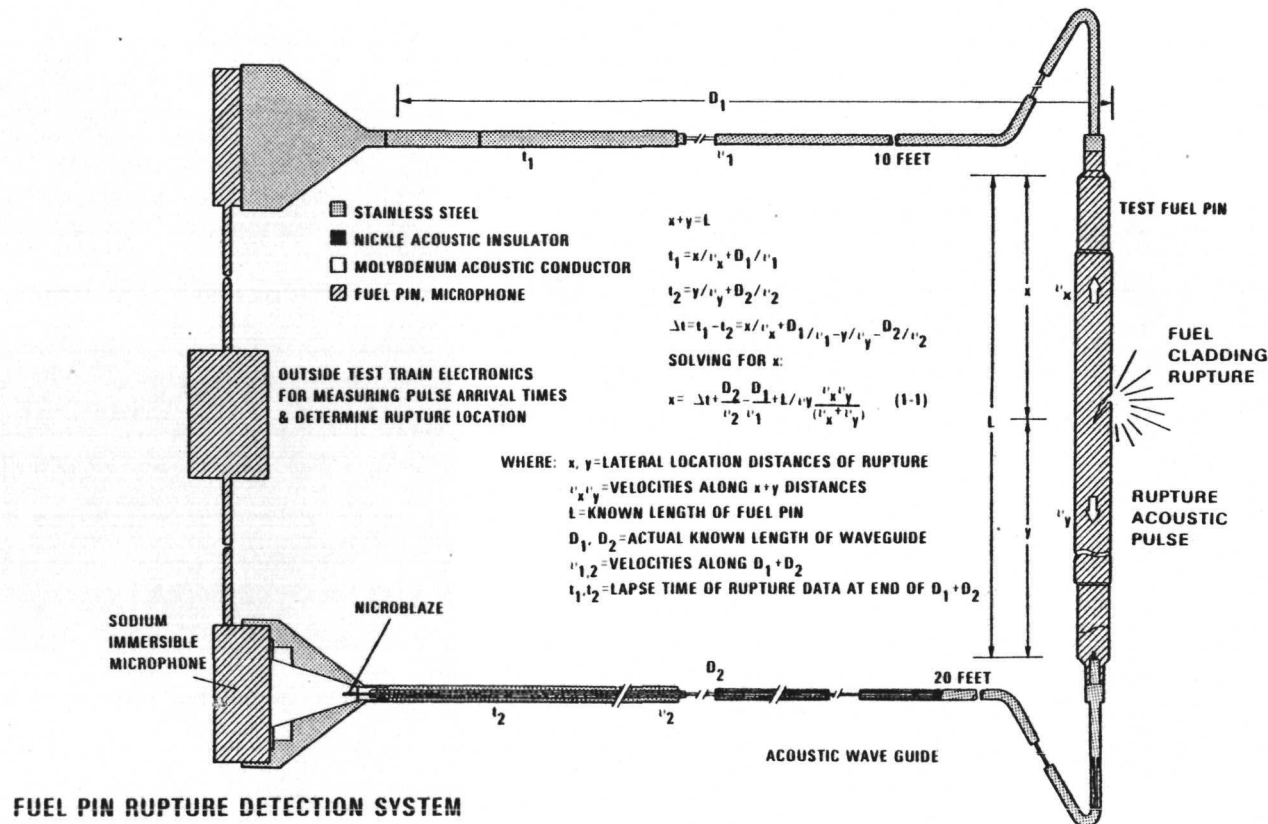
The maximum uncertainty δ_x in rupture location x is obtained by taking a total differential of equation (1-1):

$$\delta_{x_{\max*}} = \left[\delta(\Delta t) - \frac{D_2}{v_2^2} \delta v_2 + \frac{D_1}{v_1^2} \delta v_1 - \frac{L}{v_y^2} \delta v_y \right] \left[\frac{v_x^2 \delta v_y + v_y^2 \delta v_x}{(v_x + v_y)^2} \right] \quad (1-2)$$

δv = change in velocity due to differential temperature

One can see from equation (1-2), that the higher the acoustic velocity in the waveguide (v_1 and v_2), the smaller the uncertainty in the location of the rupture, provided δv_1 is about the same [$\sim 3\%$ per 810^0K (1000^0F)].

* For maximum uncertainty take all (-) terms as (+).



HEDL 8006-155.1

FIGURE 3. Fuel Pin Rupture Location Relationships.

Using these relationships and applying them to the properties of beryllium:

$$\frac{\delta_v}{v^2} = \frac{0.0128}{(0.406)^2} = 0.074$$

In comparison, using tantalum:

$$\frac{\delta_v}{v^2} = \frac{0.00387 \text{ in/sec}}{(0.129 \text{ in/sec})^2} = 0.23$$

Beryllium is 30 percent lower in possible error than tantalum.

2.1.1.1 Temperature Gradient Effects On the Acoustic Waveguide

Each length of acoustic waveguide D_1 and D_2 will vary in length, and possess various temperature gradients. As temperature changes, acoustic velocities will change, changing pulse arrival times at the microphones, which results in an error in the value of Δt . The following calculation considers a worst case situation:

a) Consider approximate velocity of sound in Tantalum

$$= 4084.3 \text{ m/sec (13,400 ft/sec)}$$

$$= 0.409 \text{ cm/sec (.161 in/sec)}$$

$$\text{Transit time of Tantalum} = 1/V = 0.409 = 2.445 \mu \text{sec/cm} \\ (6.21 \mu \text{sec/in})$$

b) From Ultrasonic Thermometry for LMFBR Systems - Final Report:⁽¹⁾

For a 280^0K change in Tantalum, the change in transit time is
 $\sim 0.0787 \mu \text{sec/cm (.2 \mu sec/in.)}$.

$$c) 1/V' = 2.445 + 0.0787 = 2.52 \mu \text{sec/cm (6.41 \mu sec/in.)}$$

$$V' = 2.52 \mu \text{sec/cm} = 3,962.7 \text{ m/sec (13,001 ft/sec).}$$

d) Calculated time differential:

0.0787 μ sec/cm

Length of acoustic pipe \sim 609.6 cm (20 ft)

0.0787 μ sec/cm \cdot 609.6 cm = 48 μ sec (rupture at center of fuel pin).

e) $\Delta L = \Delta V \Delta t = (4084.3 - 3962.7) (0.048) \text{ m/sec } 10^{-3} \text{ sec}$
 $= 0.00584 \text{ m} = 0.584 \text{ cm (0.23 in) error}$
(Worst case calculation)

Temperature gradients of the acoustic waveguide will be known and, therefore, this error can be eliminated.

2.1.1.2 Temperature Effects On Stainless Steel Cladding

As temperature changes, the acoustic velocity in the stainless steel fuel cladding will change. The extreme temperature range will be 588⁰K (600⁰F) to 1089⁰K (1500⁰F). The following calculations will determine the worst case lateral error in determining rupture location if temperature gradients were neglected:

. Calculate velocities for 588⁰K (600⁰F) (v_1) and 1089⁰K (1500⁰F) (v_2):

$$v_1 = \sqrt{\frac{E_1}{\rho_1}} = \sqrt{\frac{(1.789 \times 10^6 \text{ g/cm}^2) (1 \times 10^4 \text{ cm}^2/\text{m}^2) (9.81 \text{ m/sec}^2)}{7.89 \times 10^3 \text{ g/cm}^3}}$$

$$v_1 = 4,716 \text{ m/sec (15,469 ft/sec)}$$

$$v_2 = \sqrt{\frac{E_2}{\rho_2}} = \sqrt{\frac{(1.287 \times 10^6 \text{ g/cm}^2) (1 \times 10^4 \text{ cm}^2/\text{m}^2) (9.81 \text{ m/sec}^2)}{7.67 \times 10^3 \text{ g/cm}^3}}$$

$$v_2 = 4,057 \text{ m/sec (13,316 ft/sec)}$$

NOTE: V_1 and V_2 are rod velocities (V_R), which are approximately 20 percent slower than bulk, or longitudinal velocities, (V_L). For critical angle calculations, V_L should be used; however, for this calculation, V_R will provide satisfactory results.

- Calculate ΔV : $\Delta V = 4716 \text{ m/sec} (15,469 \text{ ft/sec}) - 4059 \text{ m/sec} (13,317 \text{ ft/sec}) = 657 \text{ m/sec} (2,155 \text{ ft/sec})$
- Calculate ΔT :
Assume worst case rupture at one end.
 $L = \sim 2.44 \text{ m} (8 \text{ ft})$
Assume rupture end at 588°K (600°F) and entire length at 1089°K (1500°F).
 $T_1 = 8/V_1 = 5.172 \times 10^{-4} \text{ sec.}$
 $T_2 + 8/V_2 = 6.008 \times 10^{-4} \text{ sec.}$
 $T = .836 \times 10^{-4} \text{ sec.}$
- Calculate L :
 $\Delta L = \Delta V \Delta T = (8.36 \times 10^{-4} \text{ sec}) (657 \text{ m/sec}) = 0.0549 \text{ m}$
[(2.16 in) worst case].
Temperature gradients will be known; therefore, any error resulting from this effort can be nullified.

2.1.2 Acoustic Wave Propagation

The rupture location of the fuel pin will be determined by measuring the time difference between the two signals generated by the microphone. It is essential that the acoustic wave velocities and path lengths be precisely determined for all segments of the acoustic path. Three items are required to achieve this determination:

- Acoustic path segment lengths and materials,
- Temperatures of path segments, and
- Acoustic velocity in segments as a function of material and temperature.

The first item is determined through inspection of the system. The second item, the temperatures, are more difficult to determine but they can be measured or calculated analytically. The final item, the acoustic wave velocity, may be determined if the wave is a longitudinal wave. The acoustic wave will remain longitudinal if the waveguide conductor characteristic diameter is much smaller than the wavelength of the acoustic signal.

wavelength/diameter > 100

where: wavelength = velocity/frequency

Candidate waveguide conductors have minimum acoustic velocities of 5000 m/sec. The microphones have a sensitivity which extend up to 100 kHz. Based on a worst case analysis, the acoustic energy wave will have a minimum wavelength of 50 mm. If the acoustic conductor has a maximum diameter of 0.5 mm (0.020 in.), the wavelength to diameter ratio will be 100. As the frequency will always be less and the acoustic velocity larger, it can be assumed that the wave propagation is always longitudinal.

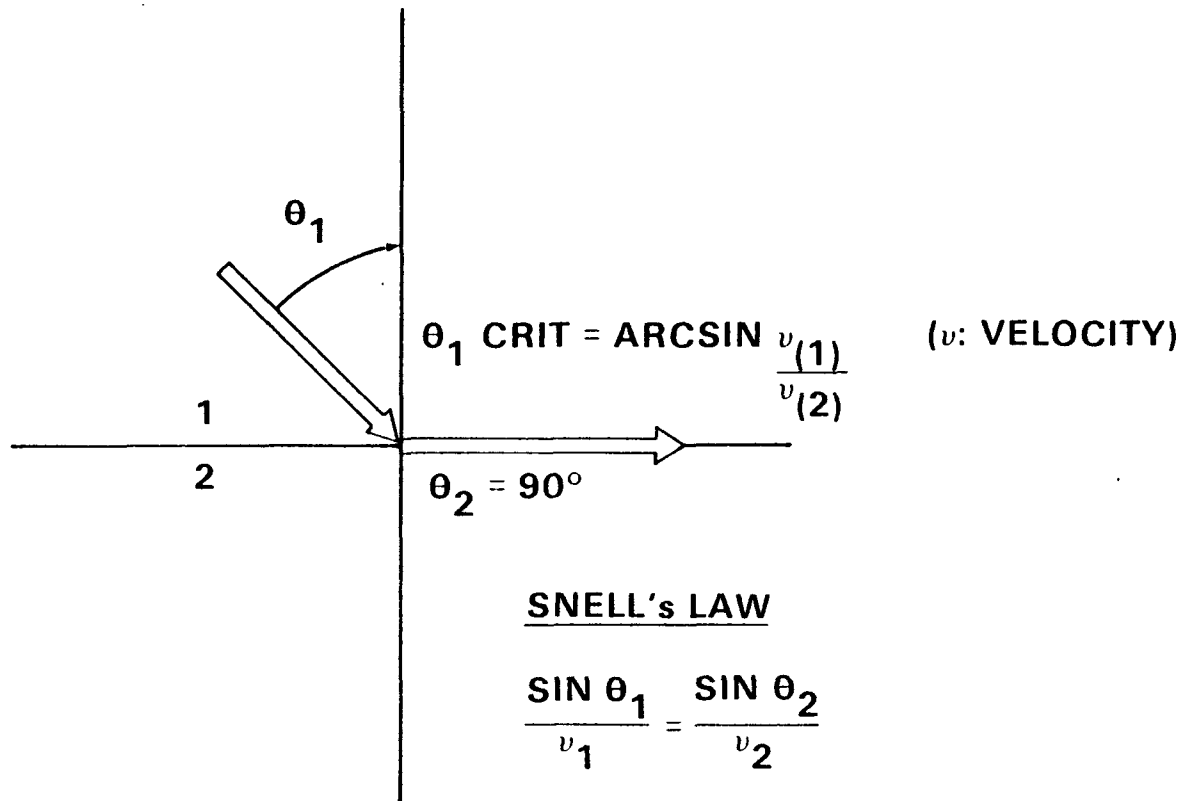
Longitudinal wave velocity may be calculated using the following relationship:

$$\text{Acoustic velocity} = \sqrt{\frac{\text{modulus of elasticity}}{\text{density}}}$$

Both the modulus and the density are determined based on the temperature and material.

2.1.3 Reflection and Critical Angle Effects On Acoustic Waveguide Design

As sound travels in a material, it will be reflected/attenuated depending on physical characteristics. These characteristics are a function of the reflection coefficient and critical angle established by boundary conditions. Figure 4 provides the critical angle definition as derived from Snell's Law.



HEDL 8005-155.2

FIGURE 4. Critical Angle Definition.

$$\text{The amplitude reflection coefficient } R = \frac{\rho_2 V_2 - \rho_1 V_1}{\rho_2 V_2 + \rho_1 V_1}$$

(ρ = density; V = velocity) ⁽³⁾.

The reflection coefficient resulting from the boundary formed by two materials is the governing factor for the magnitude of attenuation.

The critical angle is the maximum bend the center conductor can make and without creating acoustic attenuation. With no critical angle, any bend will result in substantial losses. The smaller the critical angle, the smaller the allowable bend is in the acoustic pipe. The greater the reflection coefficient, the less signal loss between two boundaries and the better the acoustic insulation.

2.1.4 Acoustic Waveguide Design

The preceding sections and the test train environment establish a number of requirements which must be satisfied in a successful acoustic waveguide. The requirements are summarized in Table 4.

The performance requirements are satisfied by careful material selections. A number of high temperature materials (also sodium compatible) were investigated with respect to their acoustic velocities. The acoustic conductor candidates are summarized in Table 5. Of the several materials available, only molybdenum and beryllium have acoustic velocities greater than that of stainless steel. Again, it is necessary to pick a conductor which has a velocity greater than that of stainless steel.

Two schemes were devised to acoustically isolate the conductor from noise generated in the test train. The first approach utilizes an acoustically attenuating material (i.e., nickel, copper) to shield out stray signals. This method is very effective in shielding the conductor; but, it also drastically attenuates the signal in the conductor as the conductor-to-shielding reflection coefficients are low (Table 6). Critical angles are non-existent

TABLE 4
ACOUSTIC WAVEGUIDE DESIGN REQUIREMENTS

Performance

Low attenuation (high reflection coefficient critical angle)
High acoustic velocity (greater than stainless steel)
High acoustic conductor wave velocity
Good isolation from test train background noise
Usable for signal frequencies of 10 to 100 kHz

Dimensions and Environment

Maximum diameter of 1.6 mm
Lengths of 3 to 6 meters
Sodium immersible
Maximum temperature = 1073°K

TABLE 5
ACOUSTIC VELOCITIES OF SELECTED MATERIALS

Beryllium (Be)	12,800 m/sec (42,000 ft/sec)
Molybdenum (Mo)	6,290 m/sec (20,670 ft/sec)
Tungsten (W)	5,180 m/sec (15,790 ft/sec)
Tantalum (Ta)	4,100 m/sec (12,500 ft/sec)
304 SS	5,640 m/sec (17,190 ft/sec)
Sodium	2,300 m/sec (7,530 ft/sec)

TABLE 6
SELECTED REFLECTION COEFFICIENTS

<u>Materials</u>	<u>R*(%)</u>
Be-Ni	36
Be-304 SS	31
Be-Air	~100
Be-Na	84
Mo-Ni	12
Mo-304 SS	18
Mo-Na	94
W-Ni	33
W-304 SS	38
Na-304 SS	91
Ni-Na	92

$$*R = \frac{\rho_2 v_2 - \rho_1 v_1}{\rho_2 v_2 + \rho_1 v_1} \quad (\rho : \text{density})$$

(v : velocity)

(Table 7). The second approach uses a wetted liquid (sodium) as the acoustic isolator. Both the molybdenum-sodium and beryllium-sodium combinations are acceptable, though the molybdenum-sodium system is less attenuating.

The sodium environment eliminates beryllium as a practical alternative for a waveguide acoustic conductor. Beryllium and molybdenum must be brazed to a stainless adapter for connection to the fuel pin end caps. A nickel-chromium-phosphorus (BNi-7) filler is used to successfully join molybdenum to stainless steel. The joint is robust and the molybdenum does not become embrittled. On the other hand, beryllium has been successfully brazed using only silver and aluminum based filler alloys which require lower temperatures and are soluble in sodium. At higher brazing temperatures (1073°K), beryllium recrystallizes and embrittles. It is also toxic, difficult to machine, expensive and difficult to obtain.

Design features of the waveguide are summarized in Table 8 and Figure 5 shows a detailed drawing of the waveguide configuration. A 0.5-mm diameter molybdenum wire is used as the acoustic conductor. (With an operating frequency of 40 kHz, the wavelength-to-diameter ratio is 300.) The conductor is brazed to a 304 SST adapter using the BNi-7 filler. The adapter is then hand gas tungsten arc (GTA) welded to the fuel pin end cap. The first ten inches of the conductor are sheathed on a 1.6 mm outer diameter (O.D.) stainless steel lower extension tube isolated from the adapter with a nickel acoustic buffer. The tube provides mechanical protection and support for conductor as it is routed out of the test section sodium flow.

The remainder of the conductor is threaded a distance of nominally 3 and 6 meters from, respectively, the upper and lower fuel pin end caps to the remotely located microphones. The acoustic conductors are also sheathed in 1.6 mm O.D. stainless steel tubes. Both the lower extension tube and the long sheath are open to the sodium, permitting wetting of both the tube and conductor surfaces. This wetted boundary reflects the fuel pin generated signals back into the conductor and shields out noise signals.

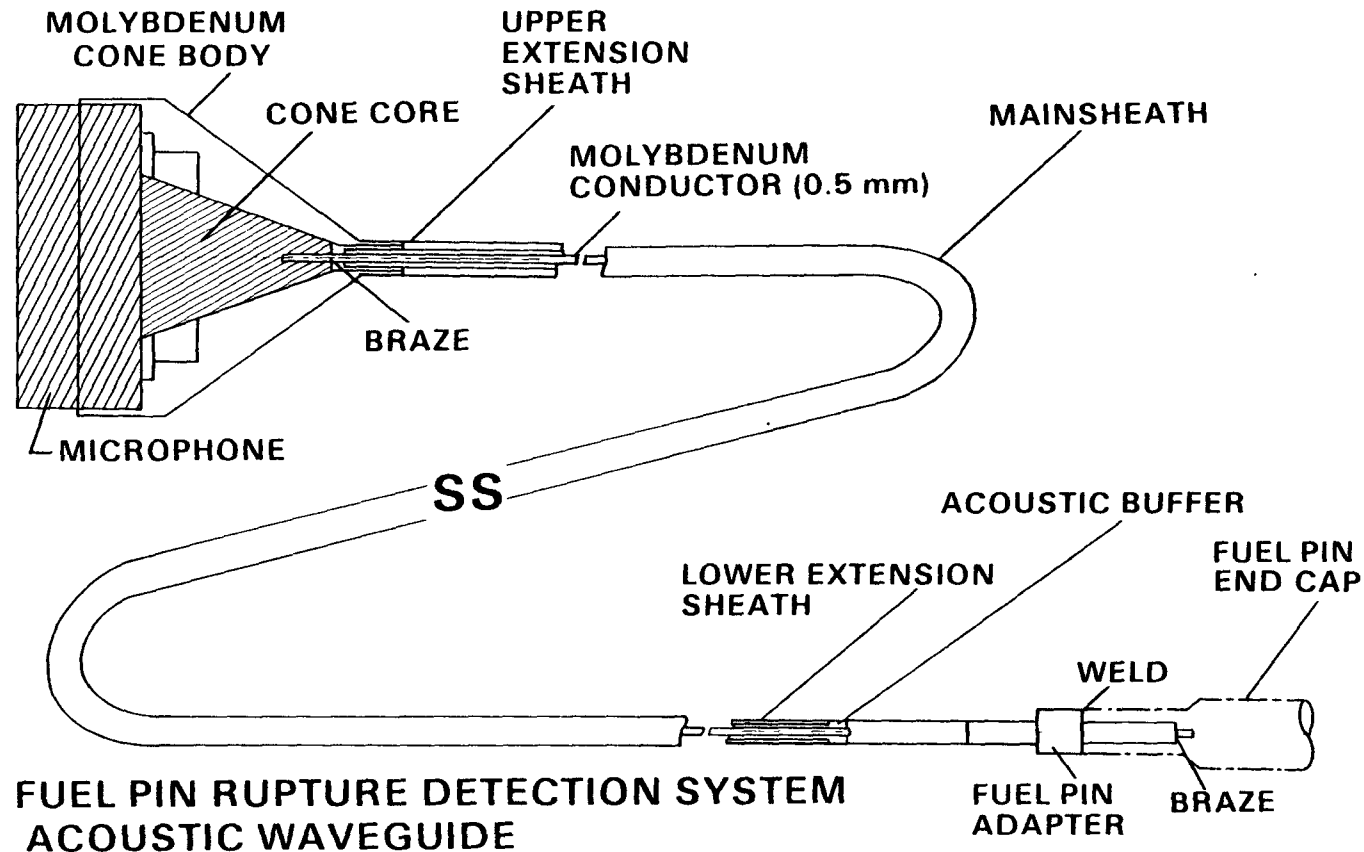
TABLE 7
CRITICAL ANGLE FOR SELECTED MATERIALS

<u>Center Acoustic Pipe Conductive</u>	<u>Outer Sheath Material</u>	<u>Crit*</u>
Beryllium	Nickel	--
Beryllium	Stainless Steel	--
Beryllium	Sodium	10.35 ⁰
Beryllium	Air	--
Molybdenum	Nickel	--
Molybdenum	Stainless Steel	--
Molybdenum	Sodium	21.45 ⁰
Molybdenum	Air	1
Stainless Steel	Sodium	24.1 ⁰

$$* \text{Crit} = \text{Arc sin } \frac{1}{2}$$

TABLE 8
ACOUSTIC WAVEGUIDE DESIGN FEATURES

Overall diameter	1.6 mm
Length	3 and 6 meters
Conductor diameter	0.5 mm
Conductor material	Molybdenum
Acoustic isolation	Wetted sodium boundary
Acoustic velocity	6200 m/sec @ 700 ⁰ K
Reflection coefficient	94%
Critical angle	20 ⁰
Maximum operating frequency	90 kHz
Maximum operating temperature	1123 ⁰ K



HEDL 8005 155 14

FIGURE 5. Acoustic Pipe Fabrication Details.

At the microphone end of the waveguide, the acoustic conductors are field brazed to molybdenum impedance matching cones using the BNi-7 filler. The cones are tapered to the maximum extent possible to allow for efficient matching of the acoustic waveform to the microphone active area. The cone diameters are 11.9 mm at the base. Stainless steel cone bodies with supportive extension sheath hold the molybdenum cones securely against the microphone surface. The cone bodies are tack welded to the microphones.

2.2 HIGH TEMPERATURE, SODIUM IMMERSIBLE MICROPHONES

Two microphones are used to convert the acoustic energy transmitted from the fuel pin by the waveguide to electrical signal. The high temperature, sodium immersible microphones fabricated by Argonne National Laboratory were selected for the transducer function.

The microphone is designed specifically for use in sodium at elevated temperatures. Table 9 lists performance specifications.⁽²⁾ The active elements in the microphone are two lithium niobate piezoelectric crystals situated between the two stainless steel faces of the microphone (Figures 6 and 7). Pressure on the face of the microphone results in the piezoelectric generation of a charge and potential between the two crystal surfaces at the central electrode. The voltage at the central electrode is transmitted by a coaxial cable. The frequency response of the microphone is presented in Figure 8.

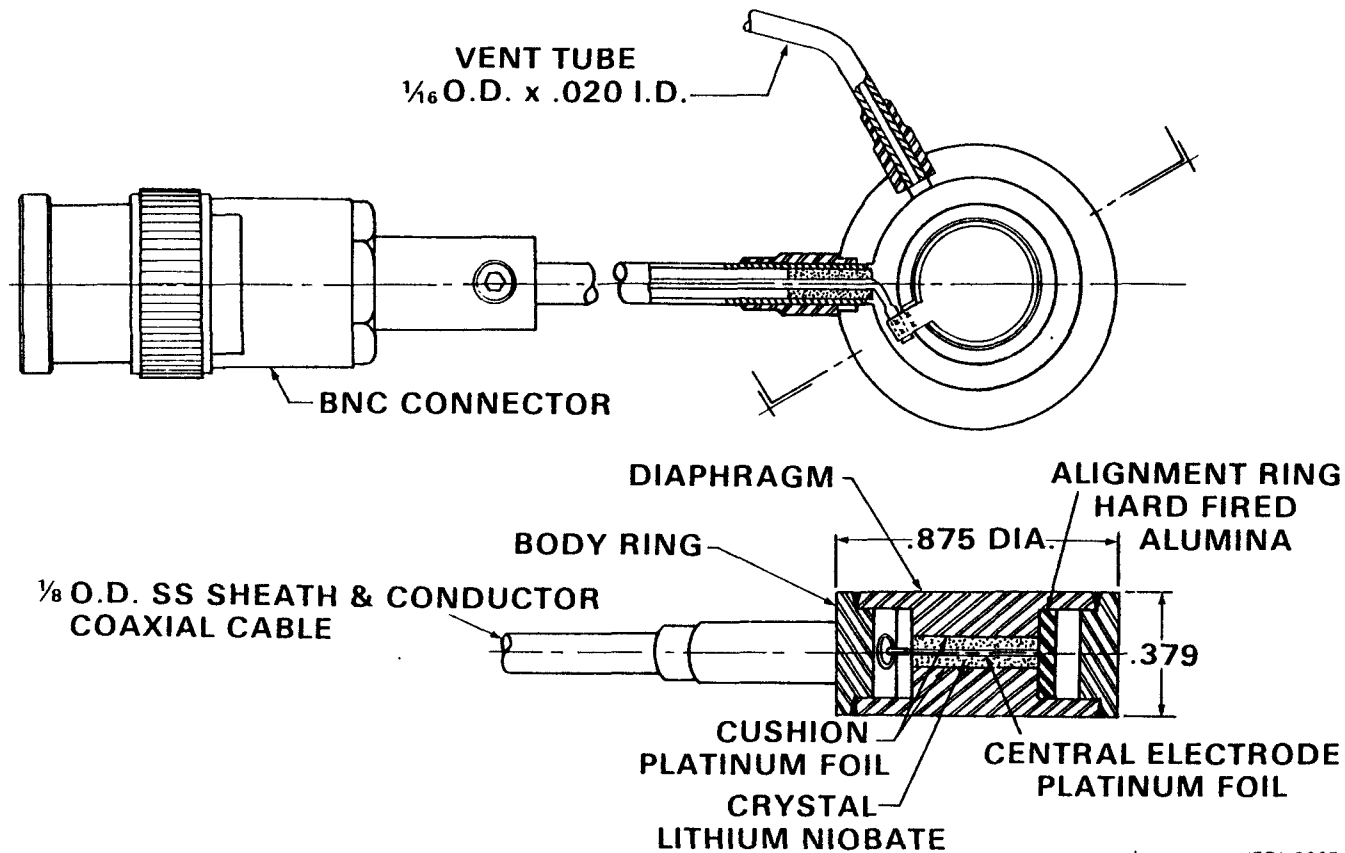
Early testing with a low temperature, wide range microphone had indicated that the majority of the acoustic energy produced by a rupture was in the 40 kHz range. The microphone is less sensitive to the frequencies (background noise) and is insensitive to higher frequencies (shear waves). The response characteristics of the microphone provide a self-filtering feature with optimum sensitivity to the rupture event frequencies.

No attempt is made to interpret the emf signal outputs of the microphones into absolute pressure or acoustic amplitude measurements. The signals are attenuated in the fuel pin and waveguides. The coupling efficiency between

TABLE 9
OPERATING CHARACTERISTICS OF ANL HIGH-TEMPERATURE MICROPHONE

Temperature*	922°K (1200°F)
Charge sensitivity	1200 - 1400 pC/bar
Frequency range	10 kHz to 100 kHz
Typical resistance at 1200°F	25 kOhms

* Higher temperatures (up to at least 978°K) cause no damage to microphone; but above 922°K, microphone resistance decreases to less than that required for operation of available charge amplifiers.



HEDL 8005-155 9

FIGURE 6. Sectional Views of ANL HT Microphone.

HIGH TEMPERATURE SODIUM IMMERSIBLE MICROPHONE

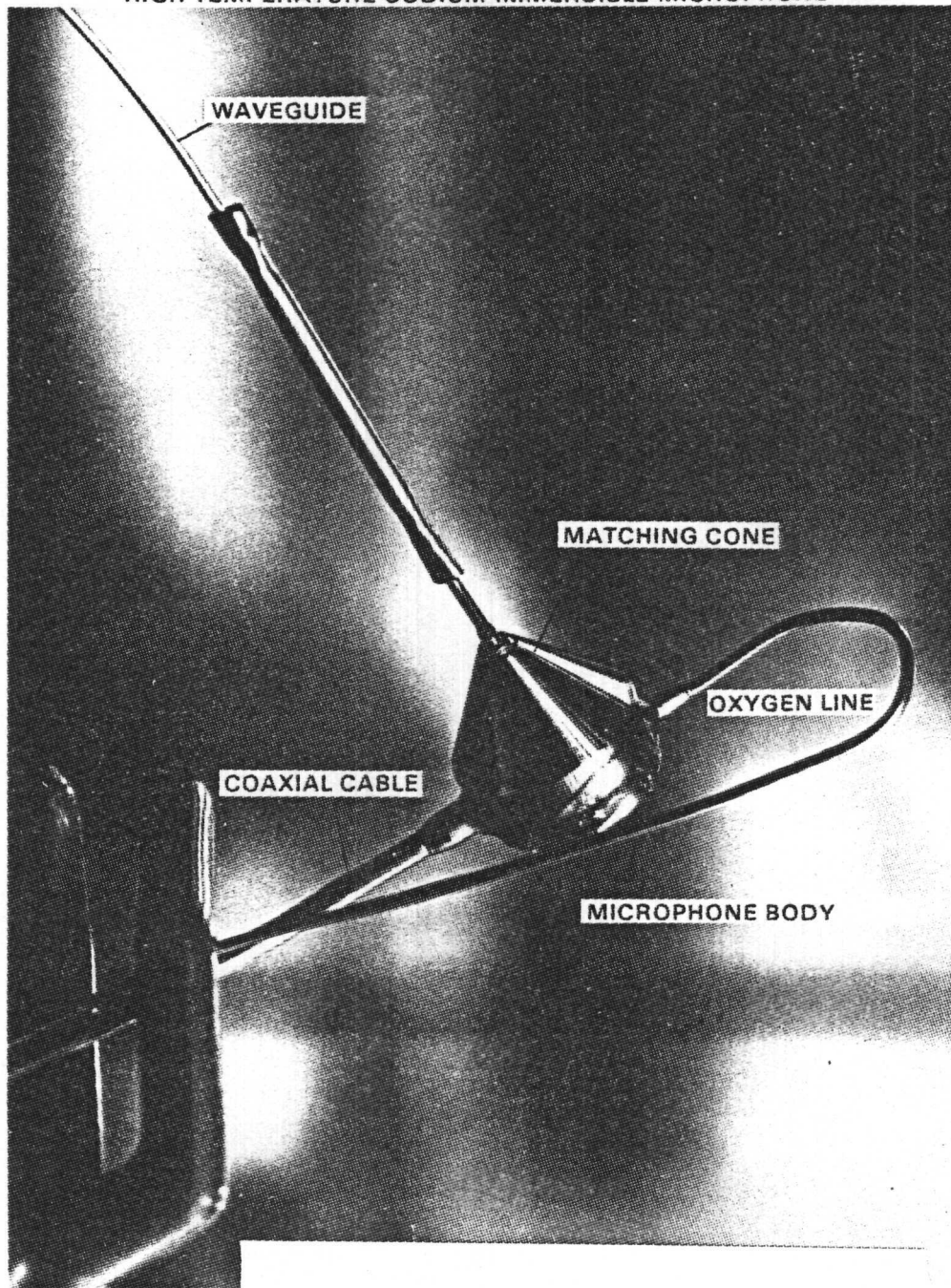
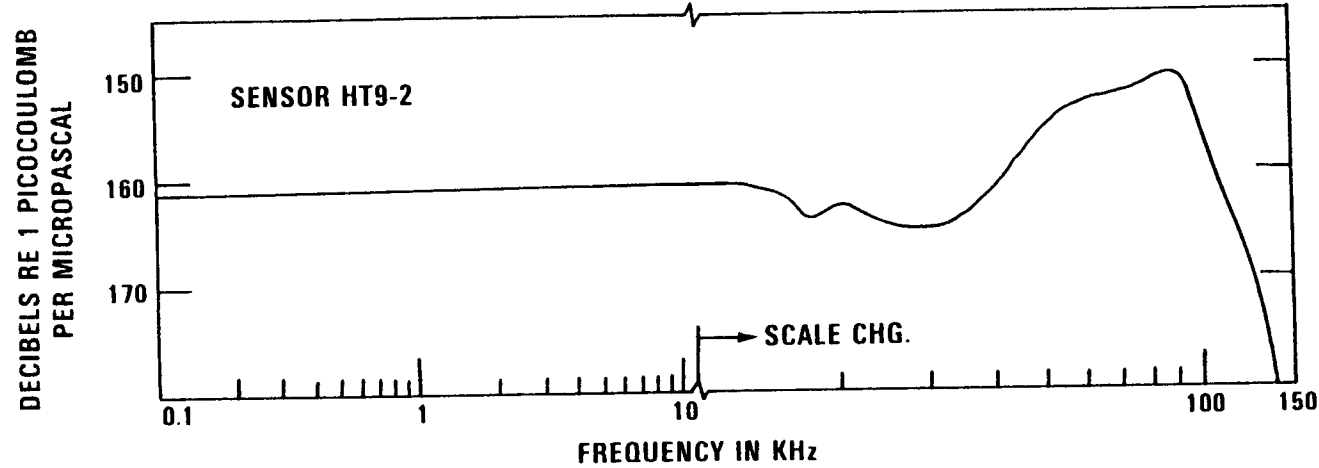


FIGURE 7. HT Microphone and Matching Cone.



HEDL 8006-155.6

FIGURE 8. Frequency Response of Typical ANL HT Microphone.

the microphones and the matching cones has not been determined. Also, the microphone ground-to-electrode resistance is very sensitive to temperature and atmosphere inside the microphone case. The emf-to-pressure calibration will vary in an undetermined manner.

Consequently, only relative (as opposed to absolute) amplitude data is considered important. Events such as rupture, boiling and fuel-cladding interactions will be adequately observed with relative measurements.

The microphone has an additionally useful feature. All piezoelectric devices may be driven by an emf signal to produce a pressure and acoustic signal. One microphone is used to pulse the acoustic circuit and the other receives the input. This is a very useful feature in that the circuit continuity can be easily tested while the system immersed in sodium.

2.3 ELECTRONICS SYSTEM DESCRIPTION

Once the acoustical rupture information is generated and satisfactorily transmitted to the microphones, it is necessary to condition and convert the signal into usable engineering information. Figure 9 shows a block diagram of the FPRDS electronics. The electronics package is broken into six stages:

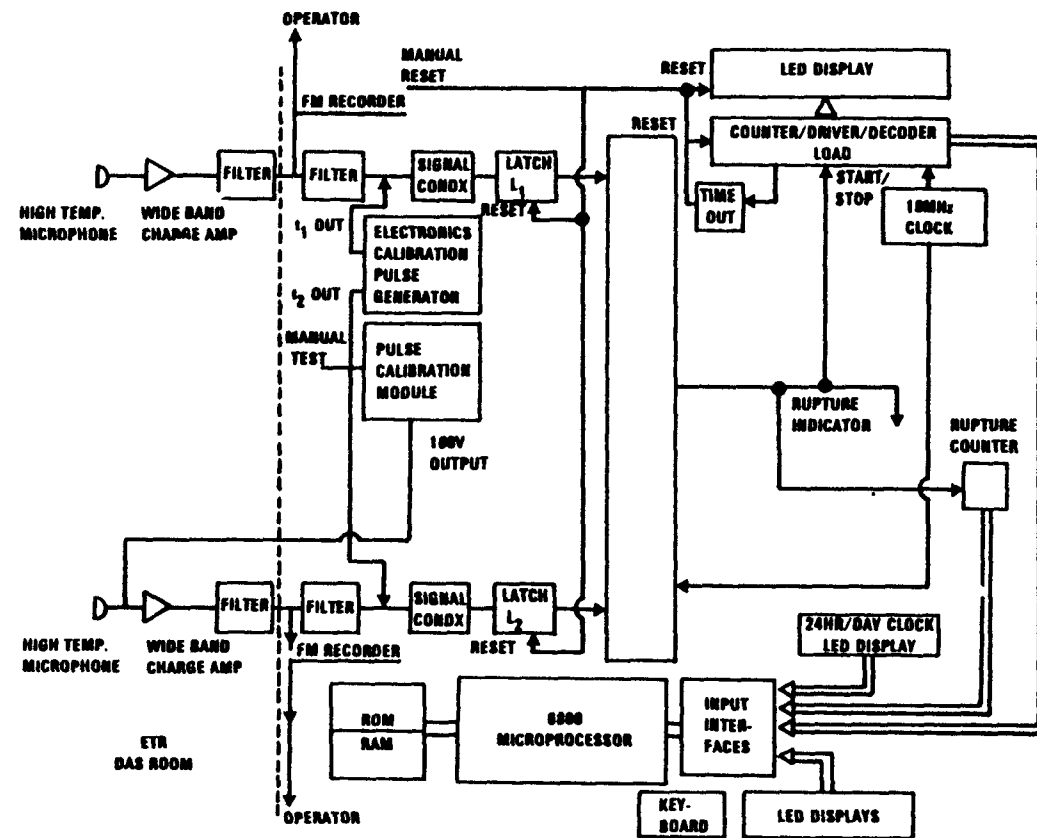
- Charge amplification
- Filtering
- FM high speed recorder (primary data collection)
- Signal conditioning
- Time Measurement Electronics (TME)
- Microprocessor based data control and collection

Charge amplifiers, filter stages, and FM recorder are commercial units. The signal conditioning, TME, and microprocessor stages involved hardware and software development. Any emf produced by the microphones as a result of the arriving acoustic rupture information, will enter the electronics package.

An Unholtz-Dickie, Model D22PMH charge amplifier amplifies the signal. Two Ithaco variable filters, model 4212, eliminate low frequency interference (60 Hz primarily). Signals from both microphones are then recorded on high speed FM recorders for playback and data analysis on strip chart recorders. The signal conditioning module provides a high amplification factor and shapes the analog signals into TTL pulses. The output of the signal conditioning is fed into the TME stage.

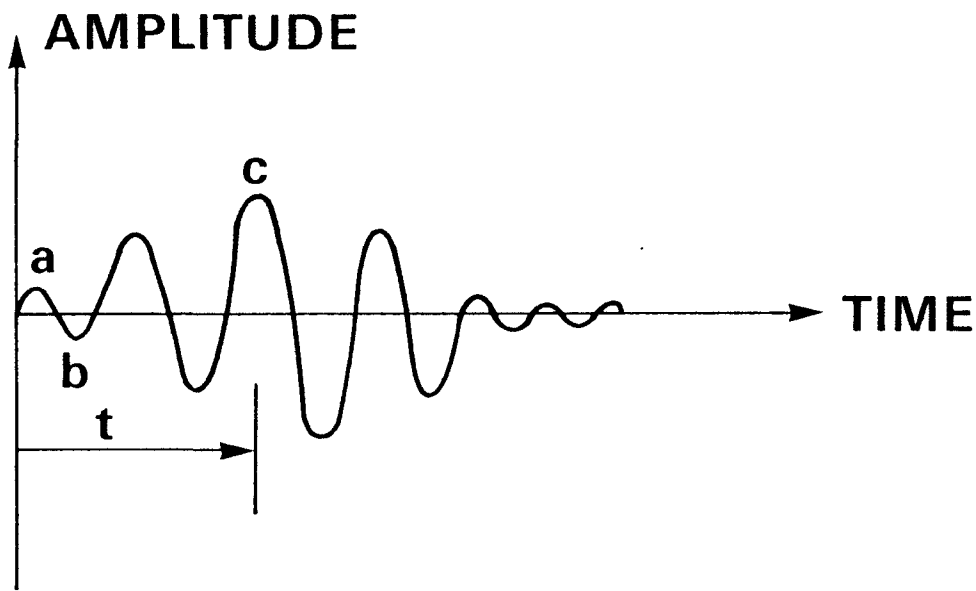
The TME circuit will be utilized to provide real-time analyses of a fuel pin rupture event. The time measurement electronics has two latched inputs. Upon receiving a signal on one input, the priority assignment circuit (PAC) will output a high TTL signal. This signal will start a 10-mHz counter and provide an interrupt to the microprocessor. When the second input receives its signal, a Δt seconds later, the PAC will drop to a low state. The 10 mHz clock will stop counting at a number representing Δt in microseconds. The microprocessor extracts this number (rupture count number) and the time from the 24-hour clock. This information is stored in a specified memory location. The microprocessor resets the whole system and readies for another set of signals. Front panel control is provided for viewing memory. The operator can extract Δt and its corresponding rupture event number and time. The TME/PAC circuitry is designed so only one set of pulses will be acted upon until a reset is provided. Once an input has received a pulse, no other signals to that input will have effect until completion of the Δt at the other input.

A typical transducer response to a pulse input is shown in Figure 10. Upon initial stimulation to a piezoelectric or similar transducer, the largest output magnitude does not occur until a time "t". This delay is a result of effects within the stimulated crystal. For the purposes of the FPRDS and obtaining an accurate Δt , initial response at "a" is very significant. At an operating frequency of 40 kHz, the time between the start of "a" and the start of "c" represents 25 microseconds. With the fuel column measuring approximately 2.44 m (8 ft), the expected time differential will be between



HEDL 8005-155.13

FIGURE 9. FPRDS Electronics Block Diagram.



HEDL 8005-155.8

FIGURE 10. Typical Transducer Response.

0 and 200 microseconds. If pulse "a" or "b" are not detected, an error of approximately \pm 15.24 cm (6 in) can result. If only "b" can be detected, a possible error of \pm 7.62 cm (3 in) can occur. Therefore, for an accuracy of less than 7.62 cm (3 in), the initial response of "a" must be detected and conditioned into a useful digital pulse by the TME circuitry.

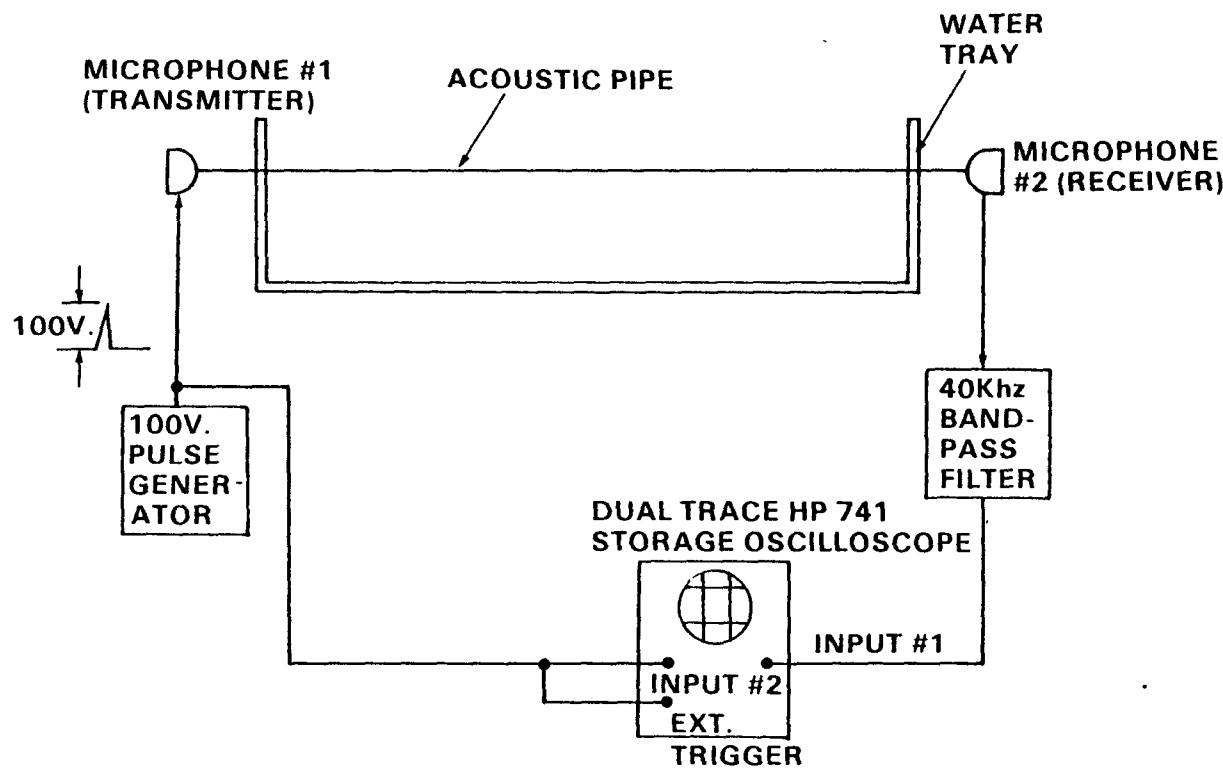
The output on the FM recorders or strip chart have the same form as that indicated in Figure 10. The initiation of events for both the upper and lower microphones are inspected manually and the time difference is determined by the operator.

3.0 TESTING RESULTS

3.1 ATTENUATION COMPARISONS FOR WAVEGUIDES

To ensure longitudinal waves will be present in the acoustic waveguide configuration at selected operating parameters, a test (repeated 20 times) was performed to measure the acoustic velocity in a 0.5 mm (20 mil) tungsten wire. A 3.04 m (10 ft) tungsten - stainless steel waveguide was fabricated with matching cones at each end. The high-temperature microphones were attached to each cone and outputs fed into charge amplifiers. The charge-amp outputs were fed into a wide 40 kHz bandpass filter. Filter outputs were connected to a dual trace, external trigger, storage oscilloscope. A step pulse was entered on the waveguide and also used to trigger the scope. Data obtained from this test yielded an acoustic velocity of 5225.2 m/sec (17,143 ft/sec). The actual table value is 5179.8 m/sec (16,994 ft/sec) for less than a one percent difference. This test showed longitudinal waves result when these parameters are present.

Figure 11 shows the test configuration for obtaining attenuation comparisons. Water was used to simulate sodium. Characteristics of water and sodium are very similar for this application.



HEDL 8005-155.12

FIGURE 11. Test Setup for Attenuation Comparisons.

Figures 12 through 14 show graphical renderings of photographs from tests performed on a 1.6 mm (0.0625 in) Mo wire using a Hewlette Packard - HP741 storage oscilloscope. Note that the water filled molybdenum wire with a stainless steel sheath, as theorized, does increase the response envelope. Also, the prototypic waveguide conductor is 0.5 mm diameter molybdenum wire. Its wavelength-to-diameter ratio is three times greater than that of the 1.6 mm wire, precluding any development of shear waves. The test configuration consisted of the low-level pulse calibration module providing the 100 v pulse to one microphone and the response viewed from the other microphone.

3.2 CALIBRATION/TEST MODULES

Two test/calibration modules were developed to aid in the electronics and acoustic pipe in-reactor checkout. The pulse generation module simply outputs a short duration, 100 volt pulse. This pulse is fed to one of the microphones. When stimulated by this high voltage, the microphone emits an acoustic pulse which travels through the acoustic pipe/fuel pin system and arrives at the other microphone. When this time delay between the transmission and reception of the acoustic pulse is measured, the system status is determined. The acoustic pipe and stainless steel fuel pins cause the time differential to be characterized due to their individual acoustic velocity characteristics. If the Δt is other than expected, a system defect may be determined by knowing the molybdenum and stainless steel velocities.

The electronics calibration pulse generator will feed a pulse into each leg of the time measurement electronics. The time differential of these pulses is known and can be varied. If the electronics is operating properly, the Δt will be displayed and logged into memory. Therefore, this test system will provide an entire electronics diagnostic check-out.



**1.588 mm (0.0625 in.)
MOLYBDENUM WIRE WITH
STAINLESS STEEL SHEATH
ANALOG RESPONSE**

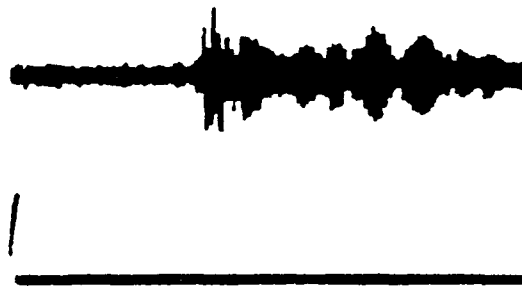


**1.588 mm (0.0625 in.)
MOLYBDENUM WIRE WITH
WATER FILLED STAINLESS
STEEL SHEATH ANALOG
RESPONSE**

INDUCED 100v PULSE

HEDL 8005-155 3

FIGURE 12. Molybdenum Wire Testing.



**1.588 mm (0.0625 in.)
MOLYBDENUM WIRE (BARE)
IN AIR ANALOG RESPONSE**

INDUCED 100v PULSE



**1.588 mm (0.0625 in.)
MOLYBDENUM WIRE (BARE)
IN WATER ANALOG RESPONSE**

INDUCED 100v PULSE

HEDL 8005-155 4

FIGURE 13. Molybdenum Wire Testing.



**1.588 mm (0.0625 in.)
MOLYBDENUM WIRE WITH
STAINLESS STEEL SHEATH
(DRY) ANALOG RESPONSE**

INDUCED 100v PULSE



**1.588 mm (0.0625 in.)
MOLYBDENUM WIRE WITH
STAINLESS STEEL SHEATH,
WATER FILLED ANALOG
RESPONSE**

INDUCED 100v PULSE

HEDL 8005-155.5

FIGURE 14. Molybdenum Wire Testing.

Assembly of the W-2 Experiment Test Train is completed. This includes fabrication of the waveguides; their attachment to the center test fuel; assembly of the fuel pin bundle; and the installation of the bundle, impedance matching cones and microphones into the test train. Acoustic continuity checks were conducted on the FPRDS as installed in the test and indicated proper functioning.

The completed W-2 test train was shipped to the ETR and was installed in the Sodium Safety Facility Loop. Sodium fill of the loop is complete and the loop is currently undergoing sodium cold trapping operations. Out-of-reactor hydraulic testing is scheduled for May 30, 1980.

Irradiation of the W-2 Experiment is scheduled for July 1980. The test will incorporate 30 full power days of steady-state irradiation and two low power practice transients. The test will conclude with the high power simulation of the FFTF 5\$/sec transient over power event.

5.0 CONCLUSION

An integrated fuel pin rupture detection system was developed based on acoustic wave propagation. Upon fuel cladding rupture, an acoustic pulse train will be emitted laterally along the pin. If the time differential of the acoustic pulse can be measured at the end caps, the actual location of the rupture can be calculated. In this analysis, remote detection of the acoustic information arriving at the fuel pin end caps was required due to the harsh environment (temperature and radiation) and limited physical space. A multi-layered acoustic waveguide has been analyzed and shown to provide an adequate transmission path for the acoustic data. High-temperature, sodium immersible microphones are used as detectors.

Temperature gradients in the acoustic pipe and temperature effects on the fuel pin were shown to have negligible effects. Several acoustic pipe configurations were discussed with applications in sodium and water.

A microprocessor based control system has been developed to collect, store, and retrieve data as well as control the entire FPRDS electronics. The software flow charts and program listing were tested and successfully utilized.

A center fuel pin in the SLSF W-2 TOP experiment has been instrumented with an FPRDS. Two waveguides, one each attached to the bottom and top of the fuel pin, will transmit acoustic information to the high temperature sodium immersible microphones. A real-time electronics package will monitor pre-transient, rupture and post-transient acoustic behavior of the fuel pin.

The FPRDS is an unique multi-scientific integrated system which required analysis in materials, electronics, acoustics, and fabrication fields.

6.0

REFERENCES

1. E. P. Papadakis, L., Lynnworth, D. Patch, and E. Carnovale, Ultrasonic Thermometry for LMFBR Systems - Final Report, AEC, NYO-3906-13, June 1972.
2. A. P. Gavin, T. T. Anderson, J. J. Janicek, "Sodium Immersible High Temperature Microphone Design Description," ANL-CT-75-30, February 1975.
3. Warren P. Mason, R. N. Thurston, Physical Acoustics, Vol. XII, Academic Press 1976, p. 348-357, New York.